

# A Robust Model for Spatiotemporal Dependencies

Fabian J. Theis<sup>a,b,\*</sup>, Peter Gruber<sup>b</sup>, Ingo R. Keck<sup>b</sup>,  
Elmar W. Lang<sup>b</sup>

<sup>a</sup>*Bernstein Center for Computational Neuroscience  
Max-Planck-Institute for Dynamics and Self-Organisation, Göttingen, Germany*

<sup>b</sup>*Institute of Biophysics, University of Regensburg, Regensburg, Germany*

---

## Abstract

Real-world data sets such as recordings from functional magnetic resonance imaging often possess both spatial and temporal structure. Here, we propose an algorithm including such spatiotemporal information into the analysis, and reduce the problem to the joint approximate diagonalization of a set of autocorrelation matrices. We demonstrate the feasibility of the algorithm by applying it to functional MRI analysis, where previous approaches are outperformed considerably.

*Key words:* blind source separation, independent component analysis, functional magnetic resonance imaging, autodecorrelation

*PACS:* 07.05.Kf, 87.61.-c, 05.40.-a, 05.45.Tp

---

## 1 Introduction

Blind source separation (BSS) describes the task of recovering an unknown mixing process and underlying sources of an observed data set. It has numerous applications in fields ranging from signal and image processing to the separation of speech and radar signals to financial data analysis. Many BSS algorithms assume either independence (independent component analysis, ICA) or diagonal autocorrelations of the sources [1,2]. Here we extend BSS algorithms based on time-decorrelation [3–8]. They rely on the fact that the data

---

\* corresponding author

*Email address:* [fabian@theis.name](mailto:fabian@theis.name) (Fabian J. Theis).

*URL:* <http://fabian.theis.name> (Fabian J. Theis).

sets have non-trivial autocorrelations so that the unknown mixing matrix can be recovered by generalized eigenvalue decomposition.

Spatiotemporal BSS in contrast to the more common spatial or temporal BSS tries to achieve both spatial and temporal separation by optimizing a joint energy function. First proposed by Stone et al. [9], it is a promising method, which has potential applications in areas where data contains an inherent spatiotemporal structure, such as data from biomedicine or geophysics including oceanography and climate dynamics. Stone’s algorithm is based on the Infomax ICA algorithm [10], which due to its online nature involves some rather intricate choices of parameters, specifically in the spatiotemporal version, where online updates are being performed both in space and time. Commonly, the spatiotemporal data sets are recorded in advance, so we can easily replace spatiotemporal online learning by batch optimization. This has the advantage of greatly reducing the number of parameters in the system, and leads to more stable optimization algorithms. We focus on so-called algebraic BSS algorithms [3,5,6,11], reviewed for example in [12], which employ generalized eigenvalue decomposition and joint diagonalization for the factorization. The corresponding learning rules are essentially parameter-free and are known to be robust and efficient [13].

In this contribution, we extend Stone’s approach by generalizing the time-decorrelation algorithms to the spatiotemporal case, thereby allowing us to use the inherent spatiotemporal structures of the data. In the experiments presented, we observe good performance of the proposed algorithm when applied to noisy, high-dimensional data sets acquired from functional magnetic resonance imaging (fMRI). We concentrate on fMRI as it is well fit for spatiotemporal decomposition due to the fact that spatial activation networks are mixed with functional and structural temporal components.

## 2 Blind source separation

We consider the following temporal *BSS* problem: Let  $\mathbf{x}(t)$  be a second-order stationary, zero-mean,  $m$ -dimensional stochastic process and  $\mathbf{A}$  a full rank matrix such that  $\mathbf{x}(t) = \mathbf{A}\mathbf{s}(t) + \mathbf{n}(t)$ . The  $n$ -dimensional source signals  $\mathbf{s}(t)$  are assumed to have diagonal *autocorrelations*  $\mathbf{R}_\tau(\mathbf{s}) := \langle \mathbf{s}(t + \tau)\mathbf{s}(t)^\top \rangle$  for all  $\tau$ , and the additive noise  $\mathbf{n}(t)$  is modeled by a stationary, temporally and spatially white zero-mean process with variance  $\sigma^2$ .  $\mathbf{x}(t)$  is observed, and the goal is to recover  $\mathbf{A}$  and  $\mathbf{s}(t)$ . Having found  $\mathbf{A}$ ,  $\mathbf{s}(t)$  can be estimated by  $\mathbf{A}^\dagger\mathbf{x}(t)$ , which is optimal in the maximum-likelihood sense, where  $\mathbf{A}^\dagger$  denotes the pseudo-inverse of  $\mathbf{A}$  and  $m \geq n$ . So the BSS task reduces to the estimation of the mixing matrix  $\mathbf{A}$ .

### 3 Separation based on time-delayed decorrelation

For  $\tau \neq 0$ , the mixture autocorrelations factorize<sup>1</sup>,

$$\mathbf{R}_\tau(\mathbf{x}) = \mathbf{A}\mathbf{R}_\tau(\mathbf{s})\mathbf{A}^\top. \quad (1)$$

This gives an indication of how to recover  $\mathbf{A}$  from  $\mathbf{x}(t)$ . The correlation of the signal part  $\tilde{\mathbf{x}}(t) := \mathbf{A}\mathbf{s}(t)$  of the mixtures  $\mathbf{x}(t)$  may be calculated as  $\mathbf{R}_0(\tilde{\mathbf{x}}) = \mathbf{R}_0(\mathbf{x}) - \sigma^2\mathbf{I}$ , provided that the noise variance  $\sigma^2$  is known. After whitening of  $\tilde{\mathbf{x}}(t)$  i.e. joint diagonalization of  $\mathbf{R}_0(\tilde{\mathbf{x}})$ , we can assume that  $\tilde{\mathbf{x}}(t)$  has unit correlation and that  $m = n$ , so  $\mathbf{A}$  is orthogonal<sup>2</sup>. If more signals than sources are observed, dimension reduction can be performed in this step thus reducing noise [14]. The *symmetrized autocorrelation* of  $\mathbf{x}(t)$ ,  $\bar{\mathbf{R}}_\tau(\mathbf{x}) := (1/2) (\mathbf{R}_\tau(\mathbf{x}) + (\mathbf{R}_\tau(\mathbf{x}))^\top)$ , factorizes as well,  $\bar{\mathbf{R}}_\tau(\mathbf{x}) = \mathbf{A}\bar{\mathbf{R}}_\tau(\mathbf{s})\mathbf{A}^\top$ , and by assumption  $\bar{\mathbf{R}}_\tau(\mathbf{s})$  is diagonal. Hence this factorization represents an eigenvalue decomposition of the symmetric matrix  $\bar{\mathbf{R}}_\tau(\mathbf{x})$ . If we furthermore assume that  $\bar{\mathbf{R}}_\tau(\mathbf{x})$  or equivalently  $\bar{\mathbf{R}}_\tau(\mathbf{s})$  has  $n$  distinct eigenvalues, then  $\mathbf{A}$  is already uniquely determined by  $\bar{\mathbf{R}}_\tau(\mathbf{x})$  except for column permutation. In addition to this separability result, a BSS algorithm namely time-delayed decorrelation [3,4] is obtained by the diagonalization of  $\bar{\mathbf{R}}_\tau(\mathbf{x})$  after whitening — the diagonalizer yields the desired separating matrix.

However, this decorrelation approach decisively depends on the choice of  $\tau$  — if an eigenvalue of  $\bar{\mathbf{R}}_\tau(\mathbf{x})$  is degenerate, the algorithm fails. Moreover, we face misestimates of  $\bar{\mathbf{R}}_\tau(\mathbf{x})$  due to finite sample effects, so using additional statistics is desirable. Therefore, Belouchrani et al [5], see also [6], proposed a more robust BSS algorithm, called *second-order blind identification (SOBI)*, jointly diagonalizing a whole set of autocorrelation matrices  $\bar{\mathbf{R}}_k(\mathbf{x})$  with varying time lags, for simplicity indexed by  $k = 1, \dots, K$ . They showed that increasing  $K$  improves SOBI performance in noisy settings [2]. Algorithm speed decreases linearly with  $K$ , so in practice  $K$  ranges from 10 to 100. Various numerical techniques for joint diagonalization exist, essentially minimizing  $\sum_{k=1}^K \text{off}(\mathbf{A}^\top \bar{\mathbf{R}}_k(\mathbf{x}) \mathbf{A})$  with respect to  $\mathbf{A}$ , where  $\text{off}$  denotes the square sum of the off-diagonal terms. A global minimum of this function is called (*approximate*) *joint diagonalizer*<sup>3</sup>, and it can be determined algorithmically for example by iterative Givens rotations [13].

<sup>1</sup>  $\mathbf{s}(t)$  and  $\mathbf{n}(t)$  can be decorrelated, so  $\mathbf{R}_\tau(\mathbf{x}) = \langle \mathbf{A}\mathbf{s}(t+\tau)\mathbf{s}(t)^\top \mathbf{A}^\top \rangle + \langle \mathbf{n}(t+\tau)\mathbf{n}(t)^\top \rangle = \mathbf{A}\mathbf{R}_\tau(\mathbf{s})\mathbf{A}^\top$ , where the last equality follows because  $\tau \neq 0$  and  $\mathbf{n}(t)$  is white.

<sup>2</sup> By assumption,  $\mathbf{R}_0(\mathbf{s}) = \mathbf{I}$  hence  $\mathbf{I} = \langle \mathbf{A}\mathbf{s}(t)\mathbf{s}(t)^\top \mathbf{A}^\top \rangle = \mathbf{A}\mathbf{R}_0(\mathbf{s})\mathbf{A}^\top = \mathbf{A}\mathbf{A}^\top$ , so  $\mathbf{A}$  is orthogonal.

<sup>3</sup> The case of perfect diagonalization i.e. the case of a zero-valued minimum occurs if and only if all matrices that are to be diagonalized commute, which is equivalent to the matrices sharing the same system of eigenvectors.

## 4 Spatiotemporal structures

Real-world data sets often possess structure in addition to the simple factorization models treated above. For example fMRI measurements contain both temporal and spatial indices so a data entry  $x = x(r_1, r_2, r_3, t)$  can depend on position  $\mathbf{r} := (r_1, r_2, r_3)$  as well as time  $t$ . More generally, we want to consider data sets  $x(\mathbf{r}, t)$  depending on two indices  $\mathbf{r}$  and  $t$ , where  $\mathbf{r} \in \mathbb{R}^n$  can be any multidimensional (spatial) index and  $t$  indexes the time axis. In practice this generalized random process is realized by a finite number of samples. For example in the case of fMRI scans we could assume  $t \in [1 : T] := \{1, 2, \dots, T\}$  and  $\mathbf{r} \in [1 : h] \times [1 : w] \times [1 : d]$ , where  $T$  is the number of scans of size  $h \times w \times d$ . So the number of spatial observations is  ${}^s m := hwd$  and the number of temporal observations  ${}^t m := T$ .

### 4.1 Temporal and spatial separation

For such multi-structured data, two methods of source separation exist. In *temporal BSS*, we interpret the data to contain a measured time series  $x_{\mathbf{r}}(t) := x(\mathbf{r}, t)$  for each spatial location  $\mathbf{r}$ . Then our goal is to apply BSS to the *temporal observation vector*  ${}^t \mathbf{x}(t) := (x_{\mathbf{r}_{111}}(t), \dots, x_{\mathbf{r}_{hwd}}(t))^{\top}$  containing  ${}^s m$  entries i.e. consisting of  ${}^s m$  spatial observations. In other words we want to find a decomposition  ${}^t \mathbf{x}(t) = {}^t \mathbf{A} {}^t \mathbf{s}(t)$  with *temporal mixing matrix*  ${}^t \mathbf{A}$  and *temporal sources*  ${}^t \mathbf{s}(t)$ , possibly of lower dimension. This contrasts to so-called *spatial BSS*, where the data is considered to be composed of  $T$  spatial patterns  $\mathbf{x}_t(\mathbf{r}) := x(\mathbf{r}, t)$ . *Spatial BSS* tries to decompose the *spatial observation vector*  ${}^s \mathbf{x}(\mathbf{r}) := (x_{t_1}(\mathbf{r}), \dots, x_{t_T}(\mathbf{r}))^{\top} \in \mathbb{R}^{{}^t m}$  into  ${}^s \mathbf{x}(\mathbf{r}) = {}^s \mathbf{A} {}^s \mathbf{s}(\mathbf{r})$  with a *spatial mixing matrix*  ${}^s \mathbf{A}$  and *spatial sources*  ${}^s \mathbf{s}(\mathbf{r})$ , possibly of lower dimension. In this case, using *multidimensional autocorrelations* considerably enhances the separation [7,8]. In order to be able to use matrix-notation, we contract the spatial multidimensional index  $\mathbf{r}$  into a one-dimensional index  $r$  by row concatenation; the full multidimensional structure will only be needed later in the calculation of the multidimensional autocorrelation. Then the data set  $x(r, t) =: x_{rt}$  can be represented by a data matrix  $\mathbf{X}$  of dimension  ${}^s m \times {}^t m$ , and our goal is to determine a source matrix  $\mathbf{S}$ , either spatially or temporally.

### 4.2 Spatiotemporal matrix factorization

Temporal BSS implies the matrix factorization  $\mathbf{X} = {}^t \mathbf{A} {}^t \mathbf{S}$ , whereas spatial BSS implies the factorization  $\mathbf{X}^{\top} = {}^s \mathbf{A} {}^s \mathbf{S}$  or equivalently  $\mathbf{X} = {}^s \mathbf{S}^{\top} {}^s \mathbf{A}^{\top}$ . Hence

$$\mathbf{X} = {}^t \mathbf{A} {}^t \mathbf{S} = {}^s \mathbf{S}^{\top} {}^s \mathbf{A}^{\top}. \quad (2)$$

So both source separation models can be interpreted as matrix factorization problems; in the temporal case restrictions such as diagonal autocorrelations are determined by the second factor, in the spatial case by the first one.

In order to achieve a spatiotemporal model, we require these conditions from both factors at the same time. In other words, instead of recovering a *single* source data set which fulfills the source conditions spatiotemporally we try to find *two* source matrices, a spatial and a temporal source matrix, and the conditions are put onto the matrices separately. So the *spatiotemporal BSS* model can be derived from equation (2) as the factorization problem

$$\mathbf{X} = {}^s\mathbf{S}^\top {}^t\mathbf{S} \quad (3)$$

with spatial source matrix  ${}^s\mathbf{S}$  and temporal source matrix  ${}^t\mathbf{S}$ , which both have (multidimensional) autocorrelations being as diagonal as possible. Diagonality of the autocorrelations is invariant under scaling and permutation, so the above model contains these indeterminacies — indeed the spatial and temporal sources can interchange scaling ( $\mathbf{L}$ ) and permutation ( $\mathbf{P}$ ) matrices,  ${}^s\mathbf{S}^\top {}^t\mathbf{S} = (\mathbf{L}^{-1}\mathbf{P}^{-1}{}^s\mathbf{S})^\top (\mathbf{L}\mathbf{P}{}^t\mathbf{S})$ , and the model assumptions still hold. The spatiotemporal BSS problem as defined in equation (3) has been implicitly proposed in [9], equation (5), in combination with a dimension reduction scheme. Here, we first operate on the general model and derive the cost function based on autodecorrelation, and only later combine this with a dimension reduction method.

## 5 Algorithmic spatiotemporal BSS

Stone et al. [9] first proposed the model from equation (3), where a joint energy function is employed based on mutual entropy and Infomax. Apart from the many parameters used in the algorithm, the involved gradient descent optimization is susceptible to noise, local minima and inappropriate initializations, so we propose a novel, more robust algebraic approach in the following. It is based on the joint diagonalization of source conditions posed not only temporally but also spatially at the same time.

### 5.1 Spatiotemporal BSS using joint diagonalization

Shifting to matrix notation, we interpret  $\bar{\mathbf{R}}_k(\mathbf{X}) := \bar{\mathbf{R}}_k({}^t\mathbf{x}(t))$  as a symmetrized temporal autocorrelation matrix, whereas  $\bar{\mathbf{R}}_k(\mathbf{X}^\top) := \bar{\mathbf{R}}_k({}^s\mathbf{x}(\mathbf{r}))$  denotes the corresponding spatial possibly multidimensional symmetrized autocorrelation matrix. Here  $k$  indexes the one- or multidimensional lags  $\tau$ . Ap-

plication of the spatiotemporal mixing model from equation (3) together with the transformation properties of the  $\mathbf{R}_k$ 's yields

$$\begin{aligned}\mathbf{R}_k(\mathbf{X}) &= \mathbf{R}_k({}^s\mathbf{S}^\top {}^t\mathbf{S}) = {}^s\mathbf{S}^\top \mathbf{R}_k({}^t\mathbf{S}) {}^s\mathbf{S} \\ \mathbf{R}_k(\mathbf{X}^\top) &= \mathbf{R}_k({}^t\mathbf{S}^\top {}^s\mathbf{S}) = {}^t\mathbf{S}^\top \mathbf{R}_k({}^s\mathbf{S}) {}^t\mathbf{S},\end{aligned}\quad (4)$$

so

$$\begin{aligned}\bar{\mathbf{R}}_k({}^t\mathbf{S}) &= {}^s\mathbf{S}^{\dagger\top} \bar{\mathbf{R}}_k(\mathbf{X}) {}^s\mathbf{S}^\dagger \\ \bar{\mathbf{R}}_k({}^s\mathbf{S}) &= {}^t\mathbf{S}^{\dagger\top} \bar{\mathbf{R}}_k(\mathbf{X}^\top) {}^t\mathbf{S}^\dagger\end{aligned}\quad (5)$$

because  ${}^*m \geq n$  and hence  ${}^*\mathbf{S}^*\mathbf{S}^\dagger = \mathbf{I}$ , where  $*$  denotes either  $\mathbf{s}$  or  $\mathbf{t}$ . By assumption the matrices  $\bar{\mathbf{R}}_k({}^*\mathbf{S})$  are as diagonal as possible. Hence we can find one of two the source sets by jointly diagonalizing either  $\bar{\mathbf{R}}_k(\mathbf{X})$  or  $\bar{\mathbf{R}}_k(\mathbf{X}^\top)$  for all  $k$ . The other source matrix can then be calculated by equation (3). However we would only be using either temporal or spatial properties, so this corresponds to only temporal or spatial BSS.

In order to include the full spatiotemporal information, we have to find diagonalizers for both  $\bar{\mathbf{R}}_k(\mathbf{X})$  and  $\bar{\mathbf{R}}_k(\mathbf{X}^\top)$  such that they satisfy the spatiotemporal model (3). For now, let us assume the (unrealistic) case of  ${}^s m = {}^t m = n$  — we will deal with the general problem using dimension reduction later. Then all matrices can be assumed to be invertible, and by model (3) we get  ${}^s\mathbf{S}^\top = \mathbf{X} {}^t\mathbf{S}^{-1}$ . Applying this to equations (5) together with an inversion of the second equation yields

$$\begin{aligned}\bar{\mathbf{R}}_k({}^t\mathbf{S}) &= {}^t\mathbf{S} \mathbf{X}^\dagger \bar{\mathbf{R}}_k(\mathbf{X}) \mathbf{X}^{\dagger\top} {}^t\mathbf{S}^\top \\ \bar{\mathbf{R}}_k({}^s\mathbf{S})^{-1} &= {}^t\mathbf{S} \quad \bar{\mathbf{R}}_k(\mathbf{X}^\top)^{-1} {}^t\mathbf{S}^\top.\end{aligned}\quad (6)$$

So we can separate the data spatiotemporally by jointly diagonalizing the set of matrices  $\{\mathbf{X}^\dagger \bar{\mathbf{R}}_k(\mathbf{X}) \mathbf{X}^{\dagger\top}, \bar{\mathbf{R}}_k(\mathbf{X}^\top)^{-1} \mid k = 1, \dots, K\}$ .

Hence the goal of achieving spatiotemporal BSS ‘as much as possible’ means minimizing the joint error term of the above joint diagonalization criterion. Moreover, either spatial or temporal separation can be favored by introducing a weighting factor  $\alpha \in [0, 1]$ . The set for approximate joint diagonalization is then defined by

$$\{\alpha \mathbf{X}^\dagger \bar{\mathbf{R}}_k(\mathbf{X}) \mathbf{X}^{\dagger\top}, (1 - \alpha) \bar{\mathbf{R}}_k(\mathbf{X}^\top)^{-1} \mid k = 1, \dots, K\}.\quad (7)$$

If  $\mathbf{A}$  is a diagonalizer of (7), then the sources can be estimated by  ${}^t\hat{\mathbf{S}} = \mathbf{A}^{-1}$  and  ${}^s\hat{\mathbf{S}} = \mathbf{A}^\top \mathbf{X}^\top$ . Joint diagonalization is usually performed by optimizing the off-diagonal criterion from above, so different scale factors in the matrices indeed yield different optima if the diagonalization cannot be achieved fully.

According to equations (6), the higher  $\alpha$  the more temporal separation is stressed. In the limit case  $\alpha = 1$  only the temporal criterion is optimized, so temporal BSS is performed, whereas for  $\alpha = 0$  a spatial BSS is calculated, although we want to remark that in contrast to the temporal case, the cost function for  $\alpha = 0$  does not equal the spatial SOBI cost function due to the additional inversion. In practice, in order to be able to weight the matrix sets using  $\alpha$  appropriately, a normalization by multiplication by a constant separately within the two sets seems to be appropriate to guarantee equal scales of the two matrix sets.

## 5.2 Dimension reduction

In principle, we may now use diagonalization of the matrix set from (7) to perform spatiotemporal BSS — but only in the case of equal dimensions. Furthermore, apart from computational issues involving the high dimensionality, the BSS estimate would be poor, simply because in the estimation either of  $\bar{\mathbf{R}}_k(\mathbf{X})$  or  $\bar{\mathbf{R}}_k(\mathbf{X}^\top)$  equal or less samples than signals are available. Hence dimension reduction is essential.

Our goal is to extract only  $n \ll \min\{^s m, ^t m\}$  sources. A common approach to do so is to approximate  $\mathbf{X}$  by the reduced singular value decomposition  $\mathbf{X} \approx \mathbf{U}\mathbf{D}\mathbf{V}^\top$  of  $\mathbf{X}$ , where only the  $n$  largest values of the diagonal matrix  $\mathbf{D}$  and the corresponding columns of the pseudo-orthogonal matrices  $\mathbf{U}$  and  $\mathbf{V}$  are used. Plugging this approximation of  $\mathbf{X}$  into (5) shows after some calculation<sup>4</sup> that the set of matrices from equation (7) can be rewritten as

$$\{\alpha \bar{\mathbf{R}}_k(\mathbf{D}^{1/2}\mathbf{V}^\top), (1 - \alpha)\bar{\mathbf{R}}_k(\mathbf{D}^{1/2}\mathbf{U}^\top)^{-1} \mid k = 1, \dots, K\}. \quad (8)$$

If  $\mathbf{A}$  is a joint diagonalizer of this set, we may estimate the sources by  ${}^t\hat{\mathbf{S}} = \mathbf{A}^\top\mathbf{D}^{1/2}\mathbf{V}^\top$  and  ${}^s\hat{\mathbf{S}} = \mathbf{A}^{-1}\mathbf{D}^{1/2}\mathbf{U}^\top$ . We call the resulting algorithm *spatiotemporal second-order blind identification* or *stSOBI*, generalizing the temporal SOBI algorithm.

---

<sup>4</sup> Using the approximation  $\mathbf{X} \approx (\mathbf{U}\mathbf{D}^{1/2})(\mathbf{V}\mathbf{D}^{1/2})^\top$  together with the spatiotemporal BSS model (3) yields  $(\mathbf{U}\mathbf{D}^{-1/2})^\top {}^s\mathbf{S}^\top {}^t\mathbf{S}(\mathbf{V}\mathbf{D}^{-1/2}) = \mathbf{I}$ . Hence  $\mathbf{W} := {}^t\mathbf{S}\mathbf{V}\mathbf{D}^{-1/2}$  is an invertible  $n \times n$  matrix. The first equation of (6) still holds in the more general case and we get  $\bar{\mathbf{R}}_k({}^t\mathbf{S}) = {}^t\mathbf{S}\bar{\mathbf{X}}^\dagger\bar{\mathbf{R}}_k(\bar{\mathbf{X}})\bar{\mathbf{X}}^\dagger{}^t\mathbf{S}^\top = \mathbf{W}\bar{\mathbf{R}}_k(\mathbf{D}^{1/2}\mathbf{V}^\top)\mathbf{W}^\top$ . The second equation of (6) cannot hold for  $n < {}^*m$ , but we can derive a similar result from (5), where we use  $\mathbf{W}^{-1} = \mathbf{D}^{-1/2}\mathbf{V}^\top {}^t\mathbf{S}^\dagger$ :  $\bar{\mathbf{R}}_k({}^s\mathbf{S}) = {}^t\mathbf{S}^\dagger{}^\top\bar{\mathbf{R}}_k(\mathbf{X}^\top){}^t\mathbf{S}^\dagger = \mathbf{W}^{-\top}\bar{\mathbf{R}}_k(\mathbf{D}^{1/2}\mathbf{U}^\top)\mathbf{W}^{-1}$  which we can now invert to get  $\bar{\mathbf{R}}_k({}^s\mathbf{S})^{-1} = \mathbf{W}\bar{\mathbf{R}}_k(\mathbf{D}^{1/2}\mathbf{U}^\top)^{-1}\mathbf{W}^\top$ .

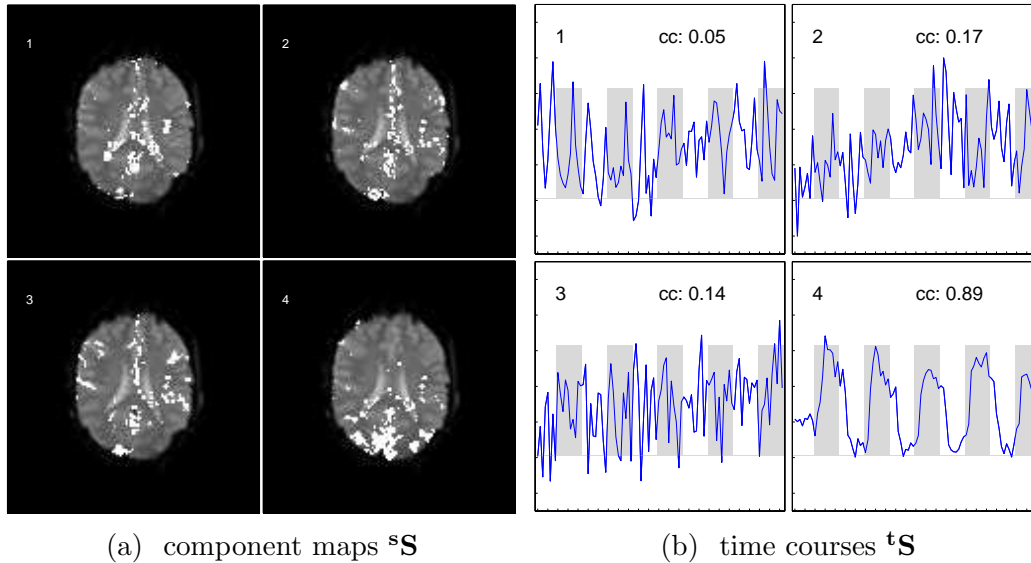


Fig. 1. fMRI analysis using stSOBI with temporal and two-dimensional spatial autocorrelations. The data was reduced to the 4 largest components. (a) shows the recovered component maps (brain background is given using a structural scan, overlaid white points indicate activation values stronger than 3 standard deviations), and (b) their time courses. Component 3 partially contains the frontal eye fields. Component 4 is the desired stimulus component, which is mainly active in the visual cortex; its time-course closely follows the on-off stimulus (indicated by the gray boxes) — their crosscorrelation lies at  $cc = 0.89$  — with a delay of roughly 6 seconds induced by the BOLD effect.

### 5.3 Implementation

In the experiments we use stSOBI with both one-dimensional and multidimensional autocovariances. Our software package<sup>5</sup> implements all the details of mdSOBI and its extension stSOBI in Matlab. In addition to Cardoso’s joint diagonalization algorithm based on iterative Givens rotations, the package contains all the files needed to reproduce the results described in this paper, with the exception of the fMRI data set.

## 6 Results

BSS, mainly based on ICA, is nowadays a quite common tool in fMRI analysis [15,16]. For this work, we analyzed the performance of stSOBI when applied to fMRI measurements. fMRI data were recorded from 10 healthy subjects performing a visual task. 100 scans ( $TR/TE = 3000/60$  ms) with 5 slices each were acquired with 5 periods of rest and 5 photic stimulation periods.

<sup>5</sup> available online at <http://fabian.theis.name/>

Stimulation and rest periods comprised 10 repetitions each i.e. 30s. Resolution was  $3 \times 3 \times 4$  mm. The slices were oriented parallel to the calcarine fissure. Photic stimulation was performed using an 8 Hz alternating checkerboard stimulus with a central fixation point and a dark background with a central fixation point during the control periods. The first scans were discarded for remaining saturation effects. Motion artifacts were compensated by automatic image alignment [17]. For visualization, we only considered a single slice (non-brain areas were masked out), and chose to reduce the data set to  $n = 4$  components by singular value decomposition.

### 6.1 *Single subject analysis*

In the joint diagonalization,  $K = 10$  autocorrelation matrices were used, both for spatial and temporal decorrelation. Figure 1 shows the performance of the algorithm for equal spatiotemporal weighting  $\alpha = 0.5$ . Although the data was reduced to only 4 components, stSOBI was able to extract the stimulus component (#4) very well; the crosscorrelation of the identified task component with the time-delayed stimulus is high ( $cc = 0.89$ ). Some additional brain components are detected, although higher  $n$  would allow for more elaborate decompositions.

In order to compare spatial and temporal models, we applied stSOBI with varying spatiotemporal weighting factors  $\alpha \in \{0, 0.1, \dots, 1\}$ . The task component was always extracted, although with different quality. In figure 2, we plotted the maximal crosscorrelation of the time courses with the stimulus versus  $\alpha$ . If only spatial separation is performed, the identified stimulus component is considerably worse ( $cc = 0.8$ ) than in the case of temporal recovery ( $cc = 0.9$ ); the component maps coincide rather well. The enhanced extraction confirms the advantages of spatiotemporal separation in contrast to the commonly used spatial-only separation. Temporal separation alone, although preferable in the presented example, often faces the problem of high dimensions and low sample number, so an adjustable weighting  $\alpha$  as proposed here allows for the highest flexibility.

### 6.2 *Algorithm comparison*

We then compared our analysis with some established algorithms for fMRI analysis. In order to numerically perform the comparisons, we determined the single component that is maximally autocorrelated with the known stimulus task. These components are shown in figure 3.

After some difficulties due to the many possible parameters, Stone’s stICA

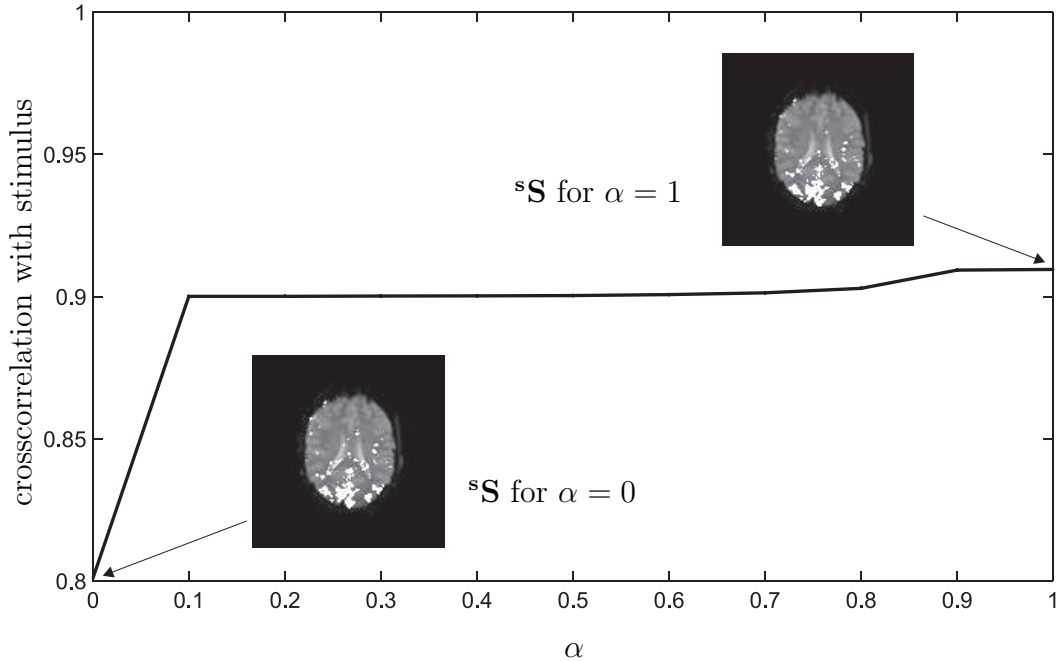


Fig. 2. Performance of stSOBI for varying  $\alpha$ . Low  $\alpha$  favors spatial separation, high  $\alpha$  temporal separation. Two recovered component maps are plotted for the extremal cases of spatial ( $\alpha = 0$ ) and temporal ( $\alpha = 1$ ) separation.

algorithm [9] was applied to the data. However, the task component could not be recovered very well — it showed some activity in the visual cortex, but with rather low temporal crosscorrelation of 0.53 with the stimulus component, which is much lower than the 0.9 of the multi-dimensional stSOBI and the 0.86 of stSOBI with one-dimensional autocovariances. We believe that this is due to convergence problems of the employed Infomax rule, and to non-trivial tuning of the many parameters involved in the algorithm. In order to test for convergence issues, we combined stSOBI and stICA by applying Stone’s local stICA algorithm to the stSOBI separation results. Due to this careful initialization, the stICA result improved (crosscorrelation of 0.58) but was still considerably lower than the stSOBI result.

Similar results were achieved by the well-known FastICA algorithm [18], which we applied in order to identify spatially independent components. The algorithm could not recover the stimulus component (maximal crosscorrelation of 0.51, and no activity in the visual cortex). This poor result is due to the dimension reduction to only 4 components, and coincides with the decreased performance of stSOBI in the spatial case  $\alpha = 0$ . In this respect, the spatiotemporal model is obviously much more flexible, as spatiotemporal dimension reduction is able to capture the structure better than only spatial reduction.

Finally, we tested the robustness of the spatiotemporal framework by modifying the cost function. It is well-known that sources with varying source properties can be separated by modifying the source condition matrices. In-

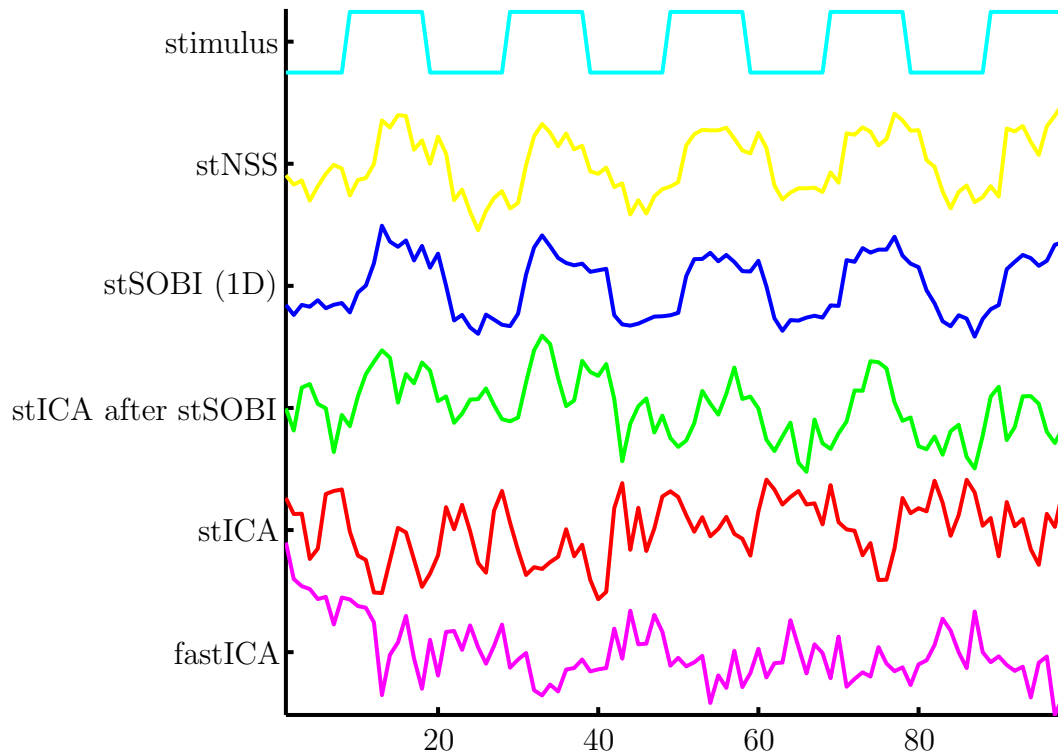


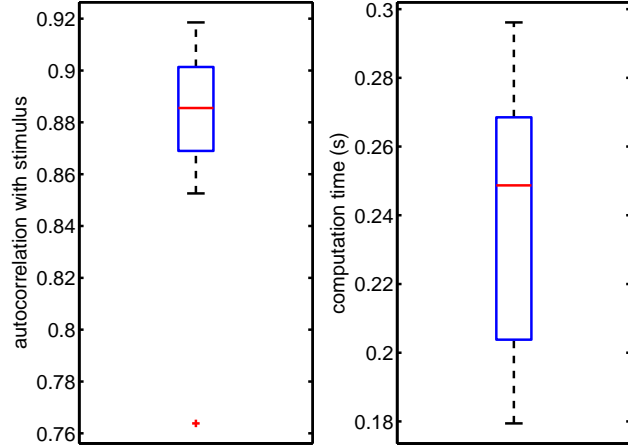
Fig. 3. Comparison of the recovered component that is maximally autocrosscorrelated with the stimulus task (top) for various BSS algorithms, after dimension reduction to 4 components. The absolute corresponding autocorrelations are 0.84 (stNSS), 0.91 (stSOBI with one-dimensional autocorrelations), 0.58 (stICA applied to separation provided by stSOBI), 0.53 (stICA) and 0.51 (fastICA).

stead of calculating autocovariance matrices, other statistics of the spatial and temporal sources can be used, as long as they satisfy the factorization from equation (1). This results in ‘algebraic BSS’ algorithms such as AMUSE [3], JADE [11], SOBI and TDSEP [5,6], reviewed for instance in [12]. Instead of performing autodecorrelation, we used the idea of the NSS-SD-algorithm (‘non-stationary sources with simultaneous diagonalization’) [19], cf. [20]: the sources were assumed to be spatiotemporal realizations of non-stationary random processes  $*s_i(t)$  with  $* \in \{t, s\}$  determining the temporal spatial or spatial direction. If we assume that the resulting covariance matrices  $\mathbf{C}(*\mathbf{s}(t))$  vary sufficiently with time, the factorization of equation (1) also holds for these covariance matrices. Hence, joint diagonalization of

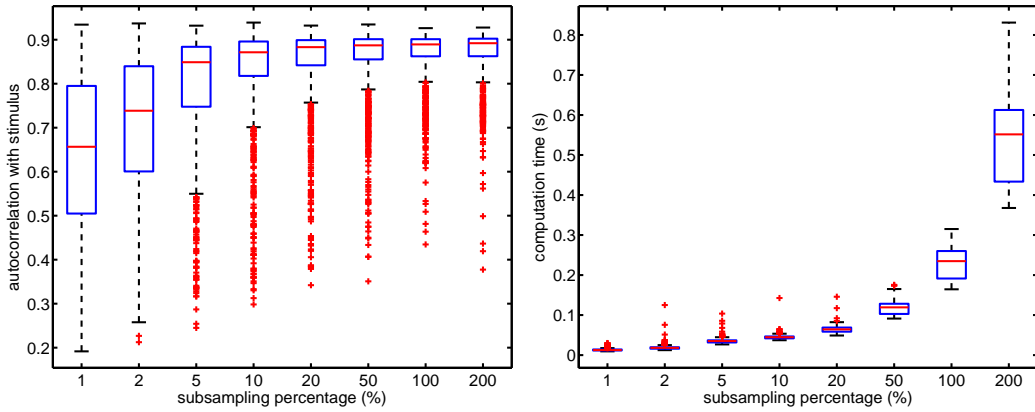
$$\{\mathbf{C}(\mathbf{t}\mathbf{x}(1)), \mathbf{C}(\mathbf{s}\mathbf{x}(1)), \mathbf{C}(\mathbf{t}\mathbf{x}(2)), \mathbf{C}(\mathbf{s}\mathbf{x}(2)), \dots\}$$

allows for the calculation of the mixing matrix. The covariance matrices are commonly estimated in separate non-overlapping temporal or spatial windows. Replacing the autocovariances in (8) by the windowed covariances, this results in the spatiotemporal NSS-SD or stNSS algorithm.

In the fMRI example, we applied stNSS using one-dimensional covariance ma-



(a) comparison of separation performance and computational effort for 10 subjects



(b) separation after subsampling      (c) computation time after subsampling

Fig. 4. Multiple subject comparison. (a) shows the algorithm performance in terms of separation quality (autocorrelation with stimulus) and computation time when compared over 100 runs and 10 subjects. (b) and (c) compare these indices after subsampling the data spatially with varying percentages.

trices and 12 windows (both temporally and spatially). Although the data exhibited only weak non-stationarities (the mean masked voxels values vary from 983 to 1000 over the 98 time steps, with a standard deviation varying from 228 to 234), the task component could be extracted rather well with a crosscorrelation of 0.80, see figure 3. Similarly, by replacing the autocorrelations with other source conditions [12], we can easily construct alternative separation algorithms.

### 6.3 Multiple subject analysis

We finish by analyzing the performance of the stSOBI algorithm for multiple subjects. As before, we applied stSOBI with dimension reduction to only  $n = 4$

sources. Here,  $K = 12$  for simplicity one-dimensional autocovariance matrices were used, both spatially and temporally. We masked the data using a fixed common threshold. In order to quantify algorithm performance, as before we determined the spatiotemporal source that had a time course with maximal autocorrelation with the stimulus protocol, and compared this autocorrelation.

In figure 4(a), we show a boxplot of the autocorrelations together with the needed computational effort. The median autocorrelation was very high with 0.89. The separation was fast with a mean computation time of 0.25s on a 1.7GHz Intel Dual Core laptop running Matlab. In order to confirm this robustness of the algorithm, we analyzed the sample-size dependence of the method by running stSOBI on subsampled data sets. The bootstrapping was performed spatially with repetition, but reordering of the samples in order to maintain spatial dependencies. Figure 4(b-c) shows the algorithm performance when varying the subsampling percentage from 1 to 200 percent, where the statistics were done over 100 runs and over the 10 subjects. Even when using only 1 percent of the samples, we achieved a median autocorrelation of 0.66, which increased at a subsampling percentage of 10% to an already acceptable value of 0.85. This confirms the robustness and efficiency of the proposed method, which of course comes from the underlying robust optimization method of joint diagonalization.

## 7 Conclusion

We have proposed a novel spatiotemporal BSS algorithm named stSOBI. It is based on the joint diagonalization of both spatial and temporal autocorrelations. Sharing the properties of all algebraic algorithms, stSOBI is easy to use, robust (with only a single parameter) and fast (in contrast to the online algorithm proposed by Stone). The employed dimension reduction allows for the spatiotemporal decomposition of high-dimensional data sets such as fMRI recordings. The presented results for such data sets show that stSOBI clearly outperforms spatial-only recovery and Stone’s spatiotemporal algorithm. Moreover, the proposed algorithm is not limited to second-order statistics, but can easily be extended to spatiotemporal ICA for example by jointly diagonalizing both spatial and temporal cumulant matrices.

## Acknowledgments

The authors gratefully acknowledge partial financial support by the DFG (GRK 638) and the BMBF (project ‘ModKog’). They would like to thank D. Auer from the MPI of Psychiatry in Munich, Germany, for providing the

fMRI data, and A. Meyer-Bäse from the Department of Electrical and Computer Engineering, FSU, Tallahassee, USA for discussions concerning the fMRI analysis. The authors thank the anonymous reviewers for their helpful comments during preparation of this manuscript.

## References

- [1] A. Hyvärinen, J. Karhunen, E. Oja, Independent component analysis, John Wiley & Sons.
- [2] A. Cichocki, S. Amari, Adaptive blind signal and image processing, John Wiley & Sons, 2002.
- [3] L. Tong, R.-W. Liu, V. Soon, Y.-F. Huang, Indeterminacy and identifiability of blind identification, *IEEE Transactions on Circuits and Systems* 38 (1991) 499–509.
- [4] L. Molgedey, H. Schuster, Separation of a mixture of independent signals using time-delayed correlations, *Physical Review Letters* 72 (23) (1994) 3634–3637.
- [5] A. Belouchrani, K. A. Meraim, J.-F. Cardoso, E. Moulines, A blind source separation technique based on second order statistics, *IEEE Transactions on Signal Processing* 45 (2) (1997) 434–444.
- [6] A. Ziehe, K.-R. Mueller, TDSEP – an efficient algorithm for blind separation using time structure, in: L. Niklasson, M. Bodén, T. Ziemke (Eds.), *Proc. of ICANN'98*, Springer Verlag, Berlin, Skövde, Sweden, 1998, pp. 675–680.
- [7] H. Schöner, M. Stetter, I. Schießl, J. Mayhew, J. Lund, N. McLoughlin, K. Obermayer, Application of blind separation of sources to optical recording of brain activity, in: *Proc. NIPS 1999*, Vol. 12, MIT Press, 2000, pp. 949–955.
- [8] F. Theis, A. Meyer-Bäse, E. Lang, Second-order blind source separation based on multi-dimensional autocovariances, in: *Proc. ICA 2004*, Vol. 3195 of LNCS, Springer, Granada, Spain, 2004, pp. 726–733.
- [9] J. Stone, J. Porrill, N. Porter, I. Wilkinson, Spatiotemporal independent component analysis of event-related fmri data using skewed probability density functions, *NeuroImage* 15 (2) (2002) 407–421.
- [10] A. Bell, T. Sejnowski, An information-maximisation approach to blind separation and blind deconvolution, *Neural Computation* 7 (1995) 1129–1159.
- [11] J. Cardoso, A. Souloumiac, Blind beamforming for non gaussian signals, *IEE Proceedings - F* 140 (6) (1993) 362–370.
- [12] F. Theis, Y. Inouye, On the use of joint diagonalization in blind signal processing, in: *Proc. ISCAS 2006*, Kos, Greece, 2006.

- [13] J. Cardoso, A. Souloumiac, Jacobi angles for simultaneous diagonalization, *SIAM J. Mat. Anal. Appl.* 17 (1) (1995) 161–164.
- [14] M. Joho, H. Mathis, R. Lamber, Overdetermined blind source separation: using more sensors than source signals in a noisy mixture, in: *Proc. of ICA 2000*, Helsinki, Finland, 2000, pp. 81–86.
- [15] M. McKeown, T. Jung, S. Makeig, G. Brown, S. Kindermann, A. Bell, T. Sejnowski, Analysis of fMRI data by blind separation into independent spatial components, *Human Brain Mapping* 6 (1998) 160–188.
- [16] I. Keck, F. Theis, P. Gruber, E. Lang, K. Specht, C. Puntonet, 3D spatial analysis of fMRI data on a word perception task, in: *Proc. ICA 2004*, Vol. 3195 of LNCS, Springer, Granada, Spain, 2004, pp. 977–984.
- [17] R. Woods, S. Cherry, J. Mazziotta, Rapid automated algorithm for aligning and reslicing pet images, *Journal of Computer Assisted Tomography* 16 (1992) 620–633.
- [18] A. Hyvärinen, E. Oja, A fast fixed-point algorithm for independent component analysis, *Neural Computation* 9 (1997) 1483–1492.
- [19] S. Choi, A. Cichocki, Blind separation of nonstationary sources in noisy mixtures, *Electronics Letters* 36 (848-849).
- [20] D.-T. Pham, J. Cardoso, Blind separation of instantaneous mixtures of nonstationary sources, *IEEE Transactions on Signal Processing* 49 (9) (2001) 1837–1848.